Targeted Observations to Improve Operational Tropical Cyclone Track Forecast Guidance

SIM D. ABERSON

Hurricane Research Division, NOAA/AOML, Miami, Florida

(Manuscript received 2 November 2001, in final form 3 January 2003)

ABSTRACT

Since 1997, the Tropical Prediction Center and the Hurricane Research Division have conducted operational synoptic surveillance missions with a Gulfstream IV-SP jet aircraft to improve numerical forecast guidance. Due to limited aircraft resources, optimal observing strategies for these missions must be developed. In the current study, the most rapidly growing modes are represented by areas of large forecast spread in the NCEP bred-vector ensemble forecasting system. The sampling strategy requires sampling of the entire target region with regularly spaced dropwindsonde observations.

Three dynamical models were employed in testing the targeting and sampling strategies. With the assimilation into the numerical guidance of all the observations gathered during the surveillance missions, only the 12-h Geophysical Fluid Dynamics Laboratory Hurricane Model forecast showed statistically significant improvement. Assimilation of only the subset of data from the subjectively found fully sampled target regions produced a statistically significant reduction of the track forecast errors of up to 25% within the critical first 2 days of the forecast. This is comparable with the cumulative business-as-usual improvement expected over 18 yr.

1. Introduction

Tropical cyclones generally exist in the data-sparse oceanic belt extending from near the equator to the subtropics. Accurate tropical cyclone track and intensity forecasting depends upon improvements to the observational network in these regions, and on accurate analysis and assimilation of these observations into numerical guidance (e.g., Riehl et al. 1956). Between 1982 and 1996, the National Oceanic and Atmospheric Administration (NOAA) Hurricane Research Division (HRD) conducted twenty ''synoptic flow'' experiments in the North Atlantic basin to gather observations in the tropical cyclone core and environment and assess their impact on the numerical guidance. The NOAA WP-3D (P-3) research aircraft released Omega dropwindsondes (ODWs) to obtain wind, temperature, and humidity profiles below about 400 hPa within 1000 km of the tropical cyclone center. Dropwindsonde observations from synoptic flow experiments produced significant improvements (16%–30% error reduction for 12–60-h forecasts) in 15 cases from 1982 to 1995 in the primary numerical guidance for the National Hurricane Center (NHC) official track forecasts (Burpee et al. 1996). These track improvements were as large as the NHC official forecast improvements obtained during the previous 20–25 yr and suggested that operational missions would be effective in reducing numerical track forecast errors.

In 1996, NOAA procured a Gulfstream IV-SP (G-IV) jet aircraft, and put it to use in operational ''synoptic surveillance'' missions in the environments of tropical cyclones threatening the continental United States, Puerto Rico, the Virgin Islands, and Hawaii. A new dropwindsonde, based on the global positioning system, was developed by the National Center for Atmospheric Research to replace the ODW (Hock and Franklin 1999). Evaluation of the first year of surveillance (1997), during which only five missions occurred, and the second year, with 19 more cases, has been reported (Aberson and Franklin 1999; Aberson 2002). Of the three dynamical track models tested, only the Geophysical Fluid Dynamics Laboratory (GFDL) Hurricane Model was improved statistically significantly by assimilation of the dropwindsonde data, and only at 12 h, too late for the issuance of new or modified hurricane watches and warnings. The amount of forecast improvement was directly related to the accuracy of the synthetic data representing the vortex in the model initial conditions and the amount of data coverage in the tropical cyclone environment. Because of limited resources, techniques to sample only those areas likely to have maximum impact on track forecasts must be developed.

Observations in particular locations in the environment of tropical cyclones have long been hypothesized

Corresponding author address: Dr. Sim D. Aberson, Hurricane Research Division, NOAA/AOML, 4301 Rickenbacker Cswy., Miami, FL 33149.
E-mail: sim.aberson@noaa.gov

to be important in forecasting storm tracks. Land-based observers and forecasters developed techniques to track and forecast tropical cyclones based on sparse environmental observations (e.g., U.S. Weather Bureau 1892; Viñes 1898). Later forecasters noted that when the approximate location of a tropical cyclone was known, observations in particular locations relative to the storm center were especially helpful in discerning the future storm track. For example, Garriott (1895) stated that the locations of surface high pressure areas to the northwest of the tropical cyclone helped in the forecasting of storm motion. Gregg (1920) felt that environmental wind observations in all directions from the tropical cyclone center, especially in the northwest quadrant, were crucial to forecasting tropical cyclone motion. Bowie (1922) commented that observations in the right-front quadrant (the northwest side of the tropical cyclone for the usual westward-moving storms) are the most important for track prediction. Jordan (1952) showed that the deep-layer wind observations extending four degrees of latitude around the storm closely corresponded to the storm motion. These inferences were not supported quantitatively until Franklin and DeMaria (1992) showed the importance of observations in the northwestern environmental quadrant of the tropical cyclone, relative to other regions, in the synoptic flow cases, and Burpee et al. (1996) showed that observations in all quadrants of the tropical cyclone environment provided impressive forecast improvements relative to guidance without the additional data. However, Aberson (2002) showed that observations obtained around the tropical cyclone did not conclusively improve forecasts more than observations only obtained in particular regions.

Other forecasters tried to find the optimal height to take observations to improve track forecasts. Gregg (1920) held that winds just above the surface steered tropical cyclones. Bowie (1922) felt that observations were most important between 3000 and 4000 m above the surface. Riehl and Shafer (1944) believed that 8000–12 000-ft winds steered immature storms, and 14 000-ft winds steered mature hurricanes. Miller and Moore (1960) held that accurate 500- or 700-hPa analyses were sufficient for accurate track prediction. Jordan (1952) introduced deep-layer steering, showing that tropical storms followed the pressure-weighted mean flow from the surface to 300 hPa. Some later studies suggested that tropical cyclones were steered by a deep-layer flow with the layer depth proportional to the storm intensity (Simpson 1971; Dong and Neumann 1986; Pike 1985; Velden and Leslie 1991), though others showed that there was no clear relationship between intensity and steering layer depth (Chen and Gray 1982; Aberson and DeMaria 1994). Aberson and Franklin (1999) showed that dropwindsonde data obtained between 150 and 400 hPa improved forecasts by approximately 10% over forecasts in which those observations were not assimilated into the numerical models, irrespective of the storm intensity.

The optimal resolution of observations in both time and space also must be deduced. Bristor (1958) suggested that observations should be taken every 6 h to optimize model improvements, though costs seem to prohibit this except with satellite data. Eliassen (1953) and Namias and Clapp (1951) both discussed the importance of global regularly spaced observations. Bristor (1958) showed that spacing between observations must be small enough to confine errors to a scale smaller than that of any particular disturbance, else numerical model errors will grow rapidly. House (1960) found that the optimal spacing not only depended upon the disturbance scale, but also on observational errors and on the data assimilation technique employed, and Aberson (2002) showed that the spreading of the impact of dropwindsonde observations around the edges of relatively well-sampled regions by current data assimilation techniques may be a factor in limitations to numerical model improvements by synoptic surveillance.

Since Aberson and Franklin (1999) showed that upper-tropospheric observations were important for improvement of tropical cyclone track forecasts, the issue of where in the vertical the observations must be taken will not be further addressed herein. Due to limited resources, only one synoptic surveillance mission each day is currently possible, so time resolution also will not be discussed. The current study is an effort to define an optimal sampling strategy to improve tropical cyclone track forecasts given that one mission per day occurs, and that the deep-layer is sampled. The next section is a review of the numerical models and the cases investigated. Sections 3 and 4 are explanations of the targeting and sampling techniques, respectively. Results and discussion are presented in sections 5 and 6, respectively.

2. Surveillance cases and numerical models

The impact on the numerical guidance of the dropwindsonde observations from the 24 synoptic surveillance missions during 1997 and 1998 was presented in Aberson (2002). Tables 1 and 2 of that manuscript, a list of the individual cases and the landfall times and locations, respectively, are reproduced here for easy reference. During each mission, the G-IV released 25–30 dropwindsondes to sample the atmosphere below flight level (near 150 hPa) at 150–200-km intervals. When one or two P-3 aircraft supplemented the G-IV missions (Table 1), 20–25 dropwindsondes were released at the same horizontal resolution from around 400 hPa. The G-IV did not penetrate the inner core of any of the tropical cyclones, though when the P-3s flew, at least one generally released dropwindsondes near the center. Air Force Reconnaissance C-130s were not involved in surveillance missions during 1997 or 1998, and any impact from Air Force aircraft missions was not investigated. HRD meteorologists aboard the G-IV and P-3 aircraft validated the wind and thermodynamic data and

TABLE 1. Synoptic surveillance missions conducted during the 1997 and 1998 hurricane seasons. The nominal time is the synoptic time for the mission (0000 UTC). The initial position and intensity are from the NHC best-track. Cases marked with superscript 1 are those in which the G-IV and one P-3 conducted the mission; those with superscript 2 are those in which the G-IV and two P-3s conducted the mission; those with superscript 3 are those in which one or two P-3s flew research missions that were not part of the synoptic surveillance mission. Superscript 4 signifies the case in which the best-track storm-motion vector was used instead of the operational value in the assessment. Superscript 5 signifies the case in which no operational vortex specification was available, and best-track data were used in the assessment.

Name	Position		Intensity	Motion vector		Nominal time
				Operational	Best-track	
Claudette[4]	34.9°N	71.8°W	17 m s^{-1}	015°/08 kt	035°/11 kt	15 Jul 1997
Erika	15.6°N	55.3°W	28 m s^{-1}	290°/17 kt	285°/17 kt	05 Sep 1997
Erika[1]	17.5°N	59.2°W	31 m s^{-1}	295°/10 kt	305°/10 kt	06 Sep 1997
Linda	21.0°N	116.5°W	64 m s^{-1}	295°/12 kt	290°/11 kt	14 Sep 1997
Linda	22.2°N	124.7°W	39 m s^{-1}	285°/11 kt	285°/10 kt	15 Sep 1997
Alex	15.9°N	51.7°W	18 m s^{-1}	275°/12 kt	275°/11 kt	01 Aug 1998
Bonnie[1]	18.7°N	61.3°W	21 m s^{-1}	285°/23 kt	290°/19 kt	21 Aug 1998
Bonnie[1]	21.1°N	67.3°W	33 m s^{-1}	295°/16 kt	300°/16 kt	22 Aug 1998
Bonnie[2]	24.8°N	71.8°W	51 m s^{-1}	335°/04 kt	340°/04 kt	24 Aug 1998
Bonnie[3]	26.9°N	73.2°W	51 m s^{-1}	330°/05 kt	330°/07 kt	25 Aug 1998
Danielle	23.9°N	66.9°W	35 m s^{-1}	290°/13 kt	290°/12 kt	29 Aug 1998
Danielle[3]	25.9°N	71.4°W	33 m s^{-1}	300°/12 kt	300°/10 kt	30 Aug 1998
Danielle[3]	27.9°N	74.1°W	36 m s^{-1}	310°/08 kt	320°/06 kt	31 Aug 1998
Earl	26.8°N	91.5°W	26 m s^{-1}	030°/09 kt	040°/13 kt	02 Sep 1998
Hermine[5]	26.9°N	90.3°W	15 m s^{-1}		315°/10 kt	17 Sep 1998
Georges[1]	13.9°N	49.0°W	46 m s^{-1}	285°/17 kt	280°/15 kt	19 Sep 1998
Georges[2]	15.7°N	54.9°W	67 m s^{-1}	285°/16 kt	285°/13 kt	20 Sep 1998
Georges[1]	18.2°N	66.3°W	46 m s^{-1}	285°/13 kt	290°/12 kt	22 Sep 1998
Georges	18.8°N	70.8°W	36 m s^{-1}	280°/14 kt	280°/12 kt	23 Sep 1998
Georges	20.5°N	74.9°W	33 m s^{-1}	295°/10 kt	320°/09 kt	24 Sep 1998
Georges	24.8°N	83.3°W	46 m s^{-1}	275°/07 kt	285°/08 kt	26 Sep 1998
Georges	27.0°N	86.5°W	49 m s^{-1}	310°/09 kt	325°/09 kt	27 Sep 1998
Mitch	15.5°N	78.4°W	51 m s^{-1}	345°/04 kt	330°/05 kt	25 Oct 1998
Mitch	16.4°N	81.0°W	67 m s^{-1}	270°/09 kt	270°/06 kt	26 Oct 1998

TABLE 2. Tropical cyclone landfalls within 120 h of the nominal time of all cases. Landfall times and locations are from NHC preliminary reports. All were during 1998.

Storm name	Nominal time	Landfall location	Landfall time
Bonnie	24 Aug	Near Wilmington, NC	0400 UTC 27 Aug
Bonnie	25 Aug	Near Wilmington, NC	0400 UTC 27 Aug
Earl	02 Sep	Near Panama Ctiy, FL	0600 UTC 03 Sep
Hermine	17 Sep	Near Cocodrie, LA	0500 UTC 20 Sep
Georges	19 Sep	3 mi SE of Falmouth, Antigua	0430 UTC 21 Sep
Georges	19 Sep	8 mi SE of Basseterre, St. Kitts	0800 UTC 21 Sep
Georges	19 Sep	20 mi SW of Fajardo, PR	2200 UTC 21 Sep
Georges	19 Sep	84 mi E of Santo Domingo, DR	1230 UTC 22 Sep
Georges	19 Sep	30 mi E of Guantanamo, Cuba	2130 UTC 23 Sep
Georges	20 Sep	3 mi SE of Falmouth, Antigua	0430 UTC 21 Sep
Georges	20 Sep	8 mi SE of Basseterre, St. Kitts	0800 UTC 21 Sep
Georges	20 Sep	20 mi SW of Fajardo, PR	2200 UTC 21 Sep
Georges	20 Sep	84 mi E of Santo Domingo, DR	1230 UTC 22 Sep
Georges	20 Sep	30 mi E of Guantanamo, Cuba	2130 UTC 23 Sep
Georges	22 Sep	84 mi E of Santo Domingo, DR	1230 UTC 22 Sep
Georges	22 Sep	30 mi E of Guantanamo, Cuba	2130 UTC 23 Sep
Georges	22 Sep	Key West, FL	1530 UTC 25 Sep
Georges	23 Sep	30 mi E of Guantanamo, Cuba	2130 UTC 23 Sep
Georges	23 Sep	Key West, FL	1530 UTC 25 Sep
Georges	24 Sep	Key West, FL	1530 UTC 25 Sep
Georges	24 Sep	Biloxi, MS	1130 UTC 28 Sep
Georges	26 Sep	Biloxi, MS	1130 UTC 28 Sep
Georges	27 Sep	Biloxi, MS	1130 UTC 28 Sep
Mitch	25 Oct	72 nm E of La Ceiba, HO	1200 UTC 29 Oct
Mitch	26 Oct	72 nm E of La Ceiba, HO	1200 UTC 29 Oct

generated standard (TEMPDROP) messages. These were transmitted to the National Centers for Environmental Prediction (NCEP) where the data were assimilated into numerical models.

To assess the impact of the dropwindsonde observations on the numerical forecasts, the version of the NCEP Global Data Assimilation System (GDAS) operational at the end of the 1998 hurricane season was used. The GDAS is composed of a quality-control algorithm, a synthetic data procedure for tropical cyclones, an analysis procedure, and the Global Spectral Model (AVN). The quality control scheme evaluates the observations by optimal interpolation and hierarchical decision-making before input to the analysis (Woollen 1991). The synthetic data procedure (Lord 1991) creates observations representative of the tropical cyclone at mandatory pressure levels between 1000 and 300 hPa within 300 km of the storm center, using the operationally estimated position, intensity, and motion, and nearby observations. The analysis scheme is the spectral statistical interpolation (Parrish and Derber 1992): the background field (the previous 6-h forecast) is combined with observations in a three-dimensional variational multivariate formalism. The forecast model's horizontal resolution is spectral triangular 126 (T126) with a Gaussian grid of 384 $\times$ 190, or approximately 1° latitude/longitude grid spacing, and the vertical coordinate extends from the surface to about 2.7 hPa with 28 unequally spaced sigma levels on a Lorenz grid (Caplan et al. 1997; Surgi et al. 1998).

The impact of dropwindsondes from the synoptic flow and surveillance missions has been assessed historically with three dynamical models using the GDAS output for initial conditions: the GFDL (Kurihara et al. 1998), VBAR (Aberson and DeMaria 1994), and AVN (Caplan et al. 1997) models. The late-1998 operational versions of these three models are used in the present study. The GDAS analysis is the direct input to AVN, whereas VBAR and GFDL modify the near-storm analysis with their own vortex specification schemes. Both GFDL and VBAR use AVN forecast fields as boundary conditions throughout the forecast duration, and neither directly ingest the dropwindsonde data. VBAR forecasts are available in the Atlantic basin only. Only GFDL provides intensity forecasts. All observations from the NCEP ''final'' archive except dropwindsonde observations were included in the GDAS. Three runs of each model were made for each mission: one with no dropwindsonde observations (NO), one with all dropwindsonde observations (AL), and the other with only those dropwindsonde observations in and around target regions (TG, as discussed below).

Some minor modifications to the operational procedures have been made for research purposes. First, postprocessed dropwindsonde observations (Hock and Franklin 1999) were used, including some that might not have been received at NCEP in real time (usually one or two extra soundings in each case). The postprocessing included automatic and manual flagging of erroneous data, interpolation where data were missing, and filtering. This method is identical to that on the aircraft, except that more time is available to examine and correct errors that may have been undetected or, more often, considered to be insignificant. Also, during postprocessing, other data sources (rawinsondes, ships, dropwindsonde data from other aircraft, etc.) permit a more thorough assessment of data quality than is possible operationally. Second, the duration of each mission was generally about 8 h, and all dropwindsonde observations from each mission were assimilated into the GDAS at the nominal mission synoptic time for consistency with previous studies and to reduce the computing requirements. All dropwindsonde observations from previous reconnaissance and surveillance missions were excluded from the data assimilation for at least 24 h before each nominal time to avoid the affects of serial correlation of tropical cyclone track forecasts (e.g., Aberson and DeMaria 1994). Assessment of the second and subsequent missions in Erika, Linda, Bonnie, Danielle, Georges, and Mitch were therefore conducted as though the previous missions had not occurred. Finally, neither aircraft reconnaissance nor visible satellite imagery were available at the mission nominal time for the Claudette case. Because the operational and best-track storm-motion vectors used by the model synthetic vortex systems differed greatly in this case, the best-track storm-motion vector was used (Aberson and Franklin 1999).

3. Target-finding technique

Numerous target-finding techniques have been tested in field experiments in the wintertime extratropics (Palmer et al. 1998). One method involves the dominant singular vectors of the integral linear propagator of the nonlinear dynamical system (Palmer et al. 1998; Buizza and Montani 1999). These singular vectors provide information about the locations of fastest perturbation growth in the model and therefore point to the regions that need to be sampled to minimize model error growth. Due to Air Route Traffic Control Center notification requirements, hurricane synoptic surveillance flights must be planned nearly 48 h before the nominal targeting time. Since the surveillance missions are designed to improve hurricane watches and warnings (24 to 48 h after the targeting time), the watch and warning time is 72 to 96 h after the initial time of the numerical guidance available at planning time. The linear propagator for tropical mesoscale phenomena such as tropical cyclones is unlikely to be appropriate on this timescale. Further, the technique is relatively expensive and requires a norm to measure the perturbation growth and a verification region where the growth is to be minimized. In the current case, targeting is conducted to improve tropical cyclone track forecasts, so no verification region is readily available, since track forecast

errors past three days are generally large (Aberson 1998).

Another adjoint-based targeting technique is the sensitivity vector. The gradient of a particular norm is transformed by the adjoint propagator to a sensitivity vector (Langland and Rohaly 1996). Again, this technique is not necessarily applicable to tropical cyclone targeting due to nonlinearity and the difficulty in creating an appropriate track norm. Another targeting technique, based on a quasi-linear inverse model, in which the tangent linear model is run with a negative time step with minor modifications, has also been tested (Pu et al. 1997; Pu and Kalnay 1999). The error dynamics also are assumed to be linear in this technique.

A fourth technique involves potential vorticity diagnosis (Appenzaler et al. 1996) of forecast failure, which has been successful in the Tropics (Shapiro 1996; Henderson et al. 1999; Shapiro and Franklin 1999). The potential vorticity inversion is capable of predicting whether any additional observations in the near-tropical cyclone environment will substantially modify the track forecast. However, the diagnosis does not supply information on specific regions near the tropical cyclone to target.

A more generalized approach, the ensemble transform technique (Bishop and Toth 1999) and the subsequent ensemble transform Kalman filter (ETKF; Bishop et al. 2001) utilizes information from any number of well-constructed ensemble forecasting systems to identify regions that, when sampled, would lead to forecast improvements. This method has been used during winter storms targeting since 1997, and became operational in 1999 (Szunyogh et al. 2000). Linear combinations of perturbations predict the forecast error variance reduction due to observations in particular areas; those areas in which the error variance reduction is greatest are to be sampled. The ETKF can identify targets given the location and error statistics of other observations; this allows for recalculation of the predicted forecast error variance reduction for the new observational network. This serial targeting mimics an entire aircraft flight, multiple aircraft, or a sequence of flights. For hurricane synoptic surveillance missions, track differences at the projected landfall time can be traced to the targeting time with the aid of the ensemble forecasts available two days before. The advantages of this technique are its relatively low cost compared with adjoint techniques, its use of nonlinear ensemble forecasts, and its ability to find target locations serially given an ensemble-based data assimilation scheme. The first skillful operational tropical cyclone track ensemble forecasting system, a 41-member orthonormalized bred-vector VBAR system, was implemented during the 2001 hurricane season (Aberson et al. 2001). The use of the ETKF and the VBAR ensemble will be reported in the future.

One other technique involves bred vectors that are related to the local Lyapunov vectors, the fastest growing modes of the system (Toth and Kalnay 1993; Lorenz and Emanuel 1998). When breeding is started, random perturbations are introduced to the model, and are repeatedly evolved and rescaled using the same nonlinear model. Growing (decaying) perturbations amplify (decay), by definition, so that only the growing modes remain after a few cycles. Since forecast fields are the first-guess fields for subsequent GDAS cycles, locations in which bred vectors are large have potentially large initial condition errors that have grown in recent forecast cycles. This technique is nonlinear and does not require an ensemble providing skillful tropical cyclone tracks, though the ensemble must provide skillful forecasts of synoptic scale features that may impact the tropical cyclone. This method is tested here for tropical cyclone targeting.

4. Targeting and sampling strategy

a. NCEP bred-vectors and increment growth

Since a goal of the surveillance missions is to improve the NCEP numerical tropical cyclone track guidance suite, the NCEP bred-vector ensemble forecasting system (Toth and Kalnay 1993) is tested. Due to operational constraints, flight tracks must be drawn the morning of the day before each planned mission, and minor adjustments can be made early the morning of the mission. The current method mimics this timetable by testing the 24-h ensemble spread forecast verifying at the nominal time of each forecast. The deep-layer mean (DLM), or 850–200 hPa, wind ensemble spread is chosen because tropical cyclones are generally steered by the environmental DLM flow, and the dropwindsondes sample this flow.

Figure 1 shows the 24-h NCEP 10-member ensemble DLM wind variance forecast at the Tropical Storm Alex mission nominal time (Table 1). The variance maximum to the north of Alex is associated with an upper-level cold low. The maximum in the southwestern Atlantic is associated with a jet streak on the southern side of the subtropical ridge. Another maximum off the middle-Atlantic United States coast corresponds to a vorticity maximum in the long-wave trough. A minimum extends along the western, southern, and eastern sides of Alex.

Figure 2a shows the increment in the DLM wind from the assimilation into the GDAS of the dropwindsonde data from the Tropical Storm Alex mission. The local ensemble spread magnitude does not correspond well to the local increment magnitude. The maximum increment to the south of Alex corresponds to an ensemble spread minimum, whereas, in the areas in which the ensemble spread is large, the increment is relatively small. After 24 h of model integration (Fig. 2b), however, the initially large increment to the south of Alex has decayed considerably, whereas the small increment to the north of Alex, where ensemble spread is large, has amplified. This example is representative of the other cases in the sample, and suggests that the regions of large ensemble variance represent areas in which drop-

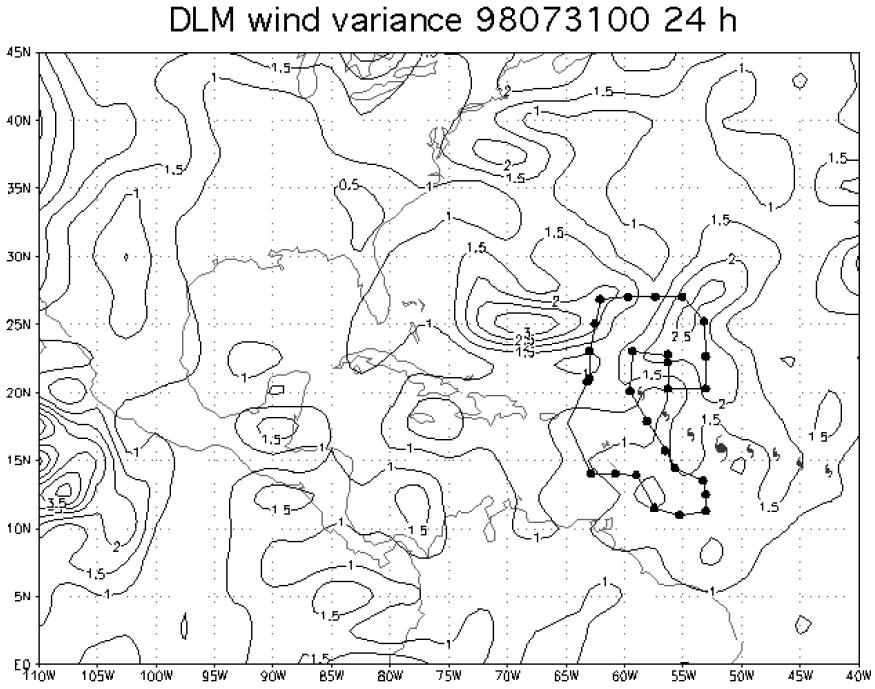

FIG. 1. Perturbation size at the nominal sampling time 0000 UTC 1 Aug 1998, from the previous day MRF ensemble forecast. The large hurricane symbol is the location of Tropical Storm Alex at the nominal time. The small hurricane symbols are the locations of Tropical Storm Alex at 12-h increments before and after the nominal time. The black dots represent the locations of dropwindsonde observations.

windsonde data will likely have growing impact on model integrations.

b. Minimization of growing errors

The GDAS is a three-dimensional variational data assimilation scheme in which the increment provided by an individual datum is quasi-isotropic; the increment is a maximum at the datum location and decreases with distance from this point. Because the synoptic surveillance missions are conducted in data-sparse oceanic regions, a relatively large increment may extend up to 1000 km from any datum location. For example, the GDAS increment provided by the dropwindsondes during the Tropical Storm Earl mission (Fig. 3a) extends into the Gulf of Tehuantepec, about 700 km from the nearest datum location. Figure 4 shows a small NCEP ensemble spread maximum in the Gulf of Tehuantepec, a larger ensemble spread maximum associated with Tropical Storm Earl in the Gulf of Mexico, and a relative minimum in the ensemble spread across Southern Mexico. After 24 h of AVN model integration (Fig. 3b), the increment near the ensemble spread minimum has decayed, and those in the ensemble spread maxima have amplified, as in the Alex example. The southern maximum is separated from the increment associated with Earl due to the decaying increment between the two growing features, and continues to grow. This increment can not be traced back directly to initial data, and so may be spurious. Such features must be minimized, especially in the area closest to the tropical cyclone, in order for the dropwindsonde data to have a large positive impact. The key is to sample features so as to limit potentially spurious increment spread into regions where increments are likely to grow. In this way, the growth of errors introduced into the model by the suboptimal data assimilation scheme are minimized. This agrees with Bergot et al. (1999), who state that with current data assimilation techniques, the entire target must be sampled, not only the extremum. These growing error modes may be one reason why the synoptic surveillance missions during 1997 and 1998 did not statistically significantly improve the numerical guidance.

c. Targeting and sampling strategy employed

The optimal targeting strategy requires both target identification and effective sampling. The NCEP bred vectors identify the target regions. The deep-layer-mean wind variance forecast verifying at the nominal time is inspected for the maxima (potential targets) closest to the tropical cyclone. The actual variance values are ignored since any variance maximum is expected to be an area of local maximum error growth. The sampling strategy requires that these targets be sampled fully at approximately the same resolution as the North American Rawinsonde Network, since this resolution has proven highly effective in improving tropical cyclone

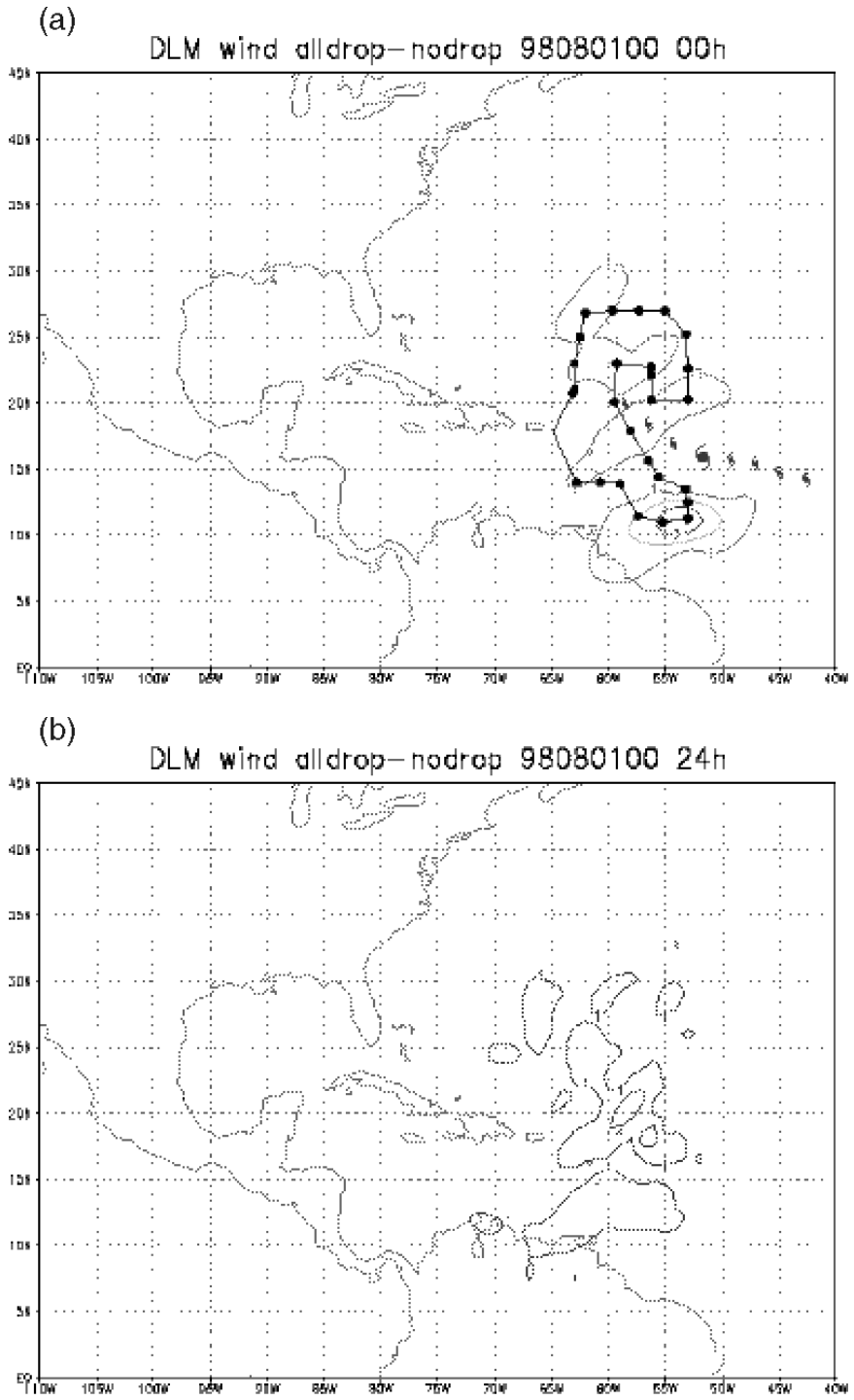

FIG. 2. Increment provided by the AL dropwindsondes in the vertically averaged 850–200-hPa winds between the AVNO and AVAL cases, 0000 UTC 1 Aug 1998, in (a) the initial conditions, and (b) after 24 h of model integration. The large hurricane symbol is the location of Tropical Storm Alex at the nominal time. The small hurricane symbols are the locations of Tropical Storm Alex at 12-h increments before and after the nominal time. The black dots represent the locations of dropwindsonde observations.

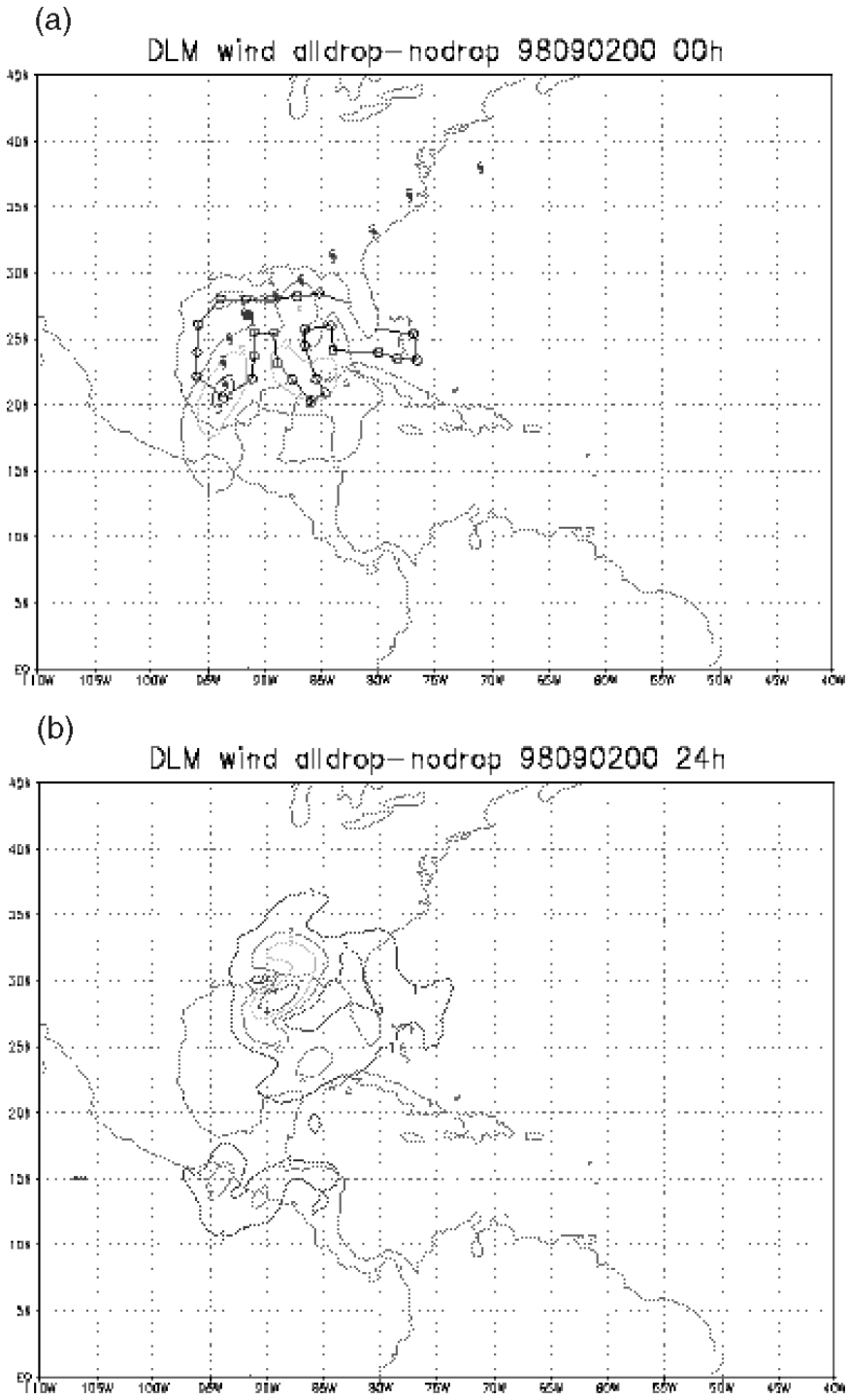

FIG. 3. Increment provided by the AL dropwindsondes in the vertically averaged 850–200-hPa winds between the AVNO and AVAL cases, 0000 UTC 2 Sep 1998, in (a) the initial conditions, and (b) after 24 h of model integration. The large hurricane symbol is the location of Tropical Storm Earl at the nominal time. The small hurricane symbols are the locations of Tropical Storm Earl at 12-h increments before and after the nominal time. The circles represent the locations of dropwindsonde observations.

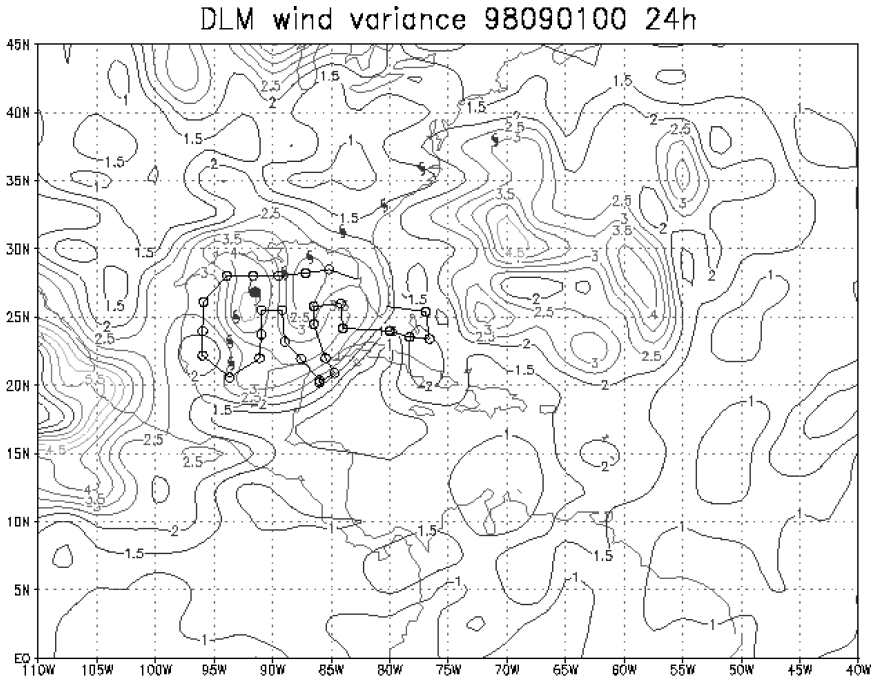

FIG. 4. Perturbation size at the nominal sampling time 0000 UTC 02 Sep 1998 from the previous day MRF ensemble forecast. The large hurricane symbol is the location of Tropical Storm Earl at the nominal time. The small hurricane symbols are the locations of Tropical Storm Earl at 12-h increments before and after the nominal time. The black circles represent the locations of dropwindsonde observations.

track forecasts (Burpee et al. 1996). Potential targets are considered to be fully sampled if dropwindsondes, with rawinsondes released from land stations, sample the extremum and the edges of the feature in an approximately regularly spaced grid. If a potential target is not fully sampled in this way, then none of the dropwindsonde data in that region are considered in the targeting sample.

Aberson (2002) has reported on the impact of the 1997 and 1998 synoptic surveillance missions with the assimilation of all the dropwindsonde observations. The current study assesses the impact of targeting by removing the data from the GDAS that fail to meet the above criterion for fully sampling targets. In this way, only the dropwindsonde data representative of the proposed targeting and sampling strategy are assimilated into the models. The NO, AL, and TG samples hereafter correspond to integrations of all three numerical models with no, all, and just the targeted dropwindsonde observations assimilated, respectively. The TG forecasts thus use only a subset of the total data accumulated during the mission.

5. Results

a. Track

Absolute track forecast errors are defined as the great-circle distance between the forecast location and the concurrent postprocessed best-track position determined by NHC after all available observations are investigated post-storm. NO and AL absolute errors for all three models are provided in Aberson (2002). Figure 5 shows the AL and TG absolute error improvements versus the NO model integrations for the three models averaged for all available cases, and the number of cases for each model, and Table 3 shows the frequency of superior performance for all three models. The comparisons within each model are homogeneous, but the intermodel comparisons are not. The number of cases varies between models because VBAR was not run for the two Linda cases in the Eastern Pacific; the Earl and Bonnie days 3 and 4 VBAR forecasts reached the model boundaries before storm dissipation; and GFDL (all Danielle) and AVN (Claudette, Bonnie day 3, Danielle day 3, and Georges day 6) predicted dissipation prematurely.

The TG improvements are larger than the AL improvements for all three models at all forecast times except for VBAR at 108 h. Among the AL versus NO comparisons, only the 12-h GFDL forecasts were improved statistically significantly at the 95% level with a paired *t*-test (e.g., Larsen and Marx 1981), with the null hypothesis that the mean of the differences is not significantly different from zero (Aberson 2002). However, the TG forecasts are statistically significantly better than the NO forecast more than half of the forecast times (Table 3). The forecast improvements within the critical

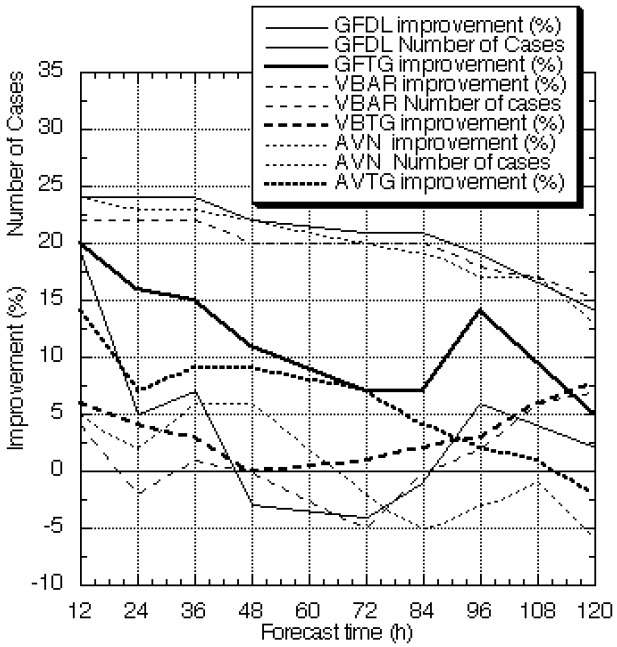

FIG. 5. Improvements in absolute track forecast errors of the GFDL, VBAR, and AVN forecasts with AL and TG dropwindsonde data over NO dropwindsonde data (lower lines), and the number of forecasts for each homogeneous comparison (upper lines).

48-h period from the initial time during which watches and warnings are raised are statistically significant in the TG sample. GFTG improvements are between 15% and 20% during the first 36 h, and no model shows average degradations with the assimilation of the TG data. Further, at a few forecast times, the TG forecasts are statistically significantly better than corresponding AL forecasts, and the reverse is not true at any forecast time. This all suggests that the targeting and sampling strategy is able to limit the impact of error growth from spurious initial increments in regions of large ensemble spread where initial condition differences are expected to grow.

b. Landfall

The most important quantifier of forecast improvement due to the assimilation of dropwindsonde data from synoptic surveillance missions is the improvement in landfall position and time forecasts. Landfall errors are investigated in the manner of Aberson (2002). Forecast positions are interpolated at half-hour intervals with splines, and the locations and times at which the tracks cross the coastline are noted. All the landfall positions and times are shown in Table 2, and the errors and improvements are in Table 4. Because landfall is a relatively rare event, these errors are not stratified by forecast time. Small distance improvements over the NO forecasts were seen in the AL sample, though none are statistically significant. By contrast, the GFTG distance forecast improvements approach 20%, and these improvements are statistically significant compared with both the GFAL and GFNO forecasts. The AVTG landfall distance errors were also improved over the AVAL and AVNO errors, and the improvements over AVNO are statistically significant. The AL landfall timing errors were substantially larger than the corresponding NO errors for all three models, though only the VBAR exhibited a statistically significant degradation. The GFTG forecasts provided a substantial timing forecast improvement over both GFNO and GFAL. The VBTG timing forecasts were slightly degraded compared with VBNO, but statistically significantly improved over VBAL forecasts. The AVTG provided small improvements compared to AVNO, and substantial improvements over AVAL in landfall time forecasts, though none of these differences are statistically significant. The TG dropwindsondes therefore not only improve the general forecast statistics relative to all the dropwindsonde data, but also improve the landfall forecast statistics.

c. Intensity

Tuleya and Lord (1997) showed modest improvements to GFDL intensity forecasts in the HRD synoptic flow cases. In the current sample, GFAL exhibits forecast intensity errors as much as 13% lower than the corresponding GFNO forecasts (Fig. 6), though only the 96-h forecast improvement is statistically significant at the 95% level. The GFTG intensity forecasts are not appreciably different from the GFAL forecasts, although

TABLE 3. Percentage of cases at each forecast time for each model in which the TG error is smaller than the NO error, the TG error is smaller than the AL error, and the AL error is smaller than the NO error. Forecast times in which the forecast error differences are statistically significant at the 95% level are shown in bold.

Model	12 h	24 h	36 h	48 h	72 h	84 h	96 h	108 h	120 h
GFTG/NO	**92**	**83**	**79**	**68**	71	71	**74**		57
GFTG/AL	46	50	58	**55**	48	43	47		33
GFAL/NO	**71**	58	63	50	62	67	63		43
VBTG/NO	**96**	**91**	73	75	65	65	56	**71**	73
VBTG/AL	82	64	55	40	60	50	56	59	67
VBAL/NO	73	64	64	60	45	55	56	65	73
AVTG/NO	**83**	74	**78**	**68**	**75**	74	65	59	40
AVTG/AL	38	44	44	41	**60**	**63**	**47**	41	50
AVAL/NO	63	61	57	50	50	45	56	53	40

TABLE 4. Landfall distance and timing forecast errors for the three models for all cases shown in Table 2. Improvements are percentage difference from the NO forecasts. Values show in boldface are statistically significantly better than at least one of the other two sets of errors.

Model name	NO distance error (km)	AL distance error (km) (improvement)	TG distance error (km) (improvement)	NO timing error (h)	AL timing error (h) (improvement)	TG timing error (h) (improvement)
GFDL	207	201 (3%)	**167 (19%)**	11.9	14.2 (−19%)	10.9 (8%)
VBAR	196	189 (4%)	192 (2%)	**11.9**	15.9 (−34%)	**12.4 (−4%)**
AVN	215	200 (7%)	**193 (10%)**	13.0	14.7 (−13%)	12.9 (1%)

the 96-h forecast is no longer statistically significantly better than the GFNO forecasts.

6. Discussion

Aberson (2002) discussed three possible reasons, besides the growth of errors introduced by suboptimal data assimilation in regions of large ensemble spread, why forecast improvements in the current sample were not as large as those in Burpee et al. (1996). Of the three, the amount of areal data coverage and the accuracy of the synthetic vortex data were shown to be important predictors of how much improvement the synoptic surveillance data provide, with the latter cause predominant. Only a small difference was seen in the forecast improvements in the sample subsets with symmetric and nonsymmetric environmental sampling, the third factor investigated. The two most important factors are examined here for the TG sample.

a. Data coverage

Aberson (2002) separated the cases into subsets depending upon how many aircraft participated in each mission (Table 1). Only those cases in which one or more P-3s were directly involved in the surveillance missions were included in the sample with more than one plane, since other research or reconnaissance missions did not augment the synoptic data coverage. The choice to involve more than one plane in the mission was not based upon any particular synoptic or environmental factors, so these factors likely play no role in the subsequent results. Though the first Georges case involved two aircraft, it was removed from the multiplane subset because both aircraft flew abbreviated missions, and the total data coverage was approximately that of a one-plane mission. The AVAL and VBAL forecasts provided substantially larger forecast improvements when dropwindsondes from one or two NOAA P-3 aircraft supplemented the data from the G-IV; the differences in the two samples were not large in the GFDL model (Aberson 2002).

The improvements to the model forecasts due to the assimilation of the dropwindsonde data in the one- and multiaircraft subsets are shown in Fig. 7 and Table 5. The GFTG forecasts in the one-plane subset were substantially better than the GFAL and GFNO forecasts, which were not very different from each other. However,

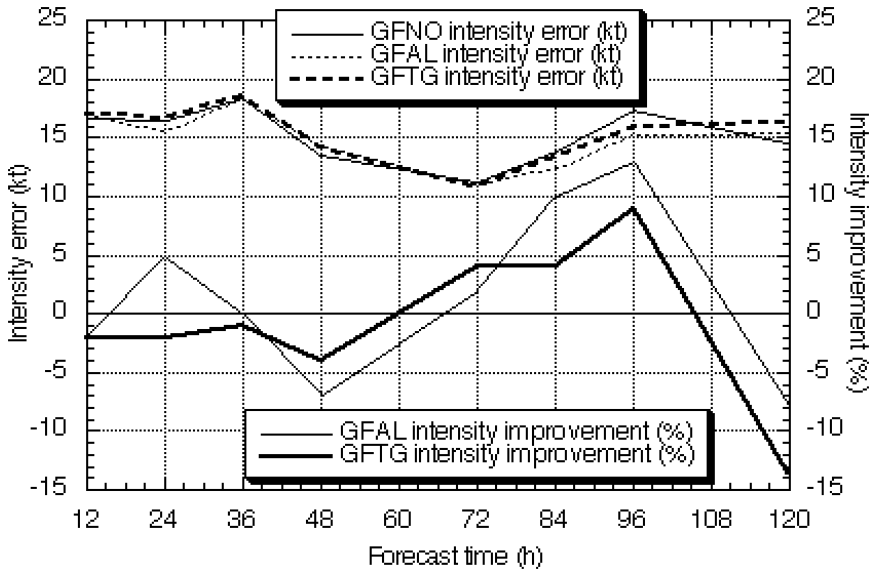

FIG. 6. Intensity error of GFDL forecasts with AL and TG dropwindsonde data over NO dropwindsonde data, and the improvements of the AL and TG forecasts over the NO forecasts.

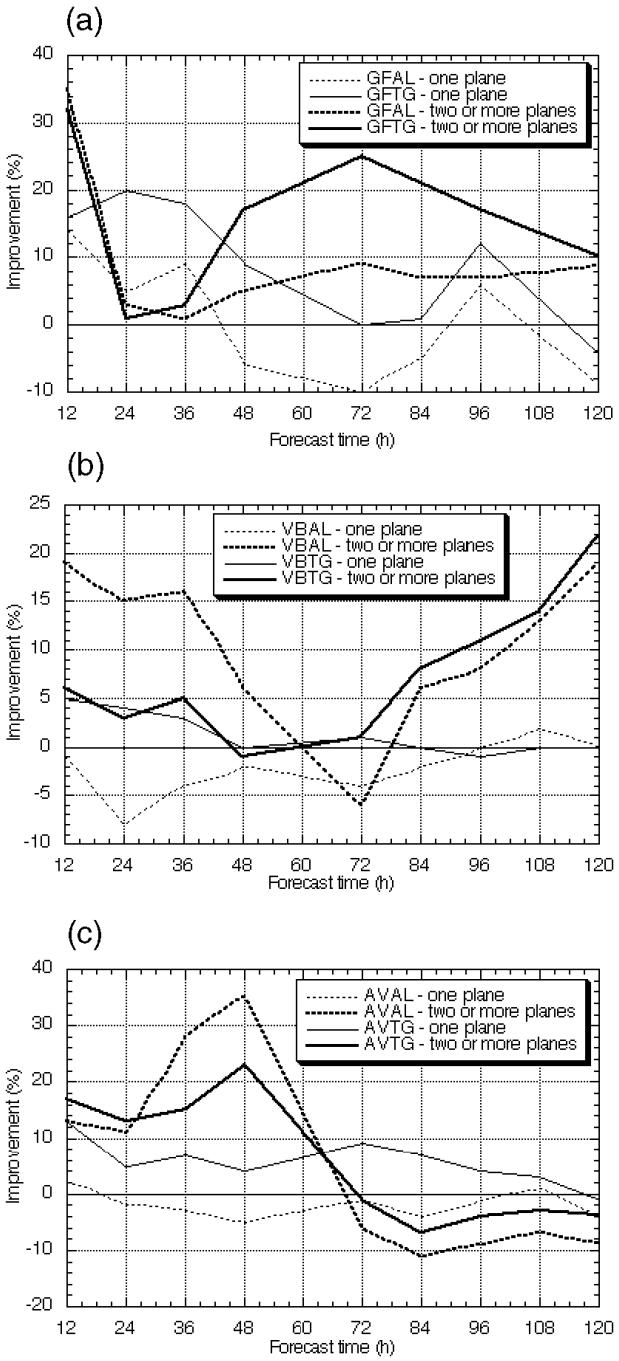

FIG. 7. Improvements of the AL and TG forecasts over the NO forecasts in those cases in which only the G-IV flew (one plane), and in those cases in which the G-IV mission was supplemented by at least one P-3 aircraft for (a) GFDL, (b) VBAR, (c) AVN.

in the multiplane subset, the GFTG forecasts were substantially better than the GFNO forecasts, though the improvements were not as large as in the one-plane sample. The GFAL improvement was half as large as that of the GFTG.

The VBTG forecasts were substantially better than the VBNO forecasts in the one-plane sample. The VBTG forecasts were also generally better than the VBAL, though the improvements were not as large. The VBAL and VBNO forecasts were not substantially different. The VBTG forecasts were substantially worse than the VBAL forecasts in the multiplane sample, though these forecasts were still an improvement to the VBNO forecasts.

The one-plane AVTG forecasts were better than the corresponding AVAL and AVNO forecasts, which were not very different from each other. In the multiplane subset, the AVAL forecasts are not significantly different from either the AVNO or the AVTG forecasts, though some of the improvements are large. The lack of significance occurs because nearly half of the sample is degraded by the dropwindsonde data. The AVTG multiplane forecasts are significantly better than the similar AVNO forecasts at 48 h.

The targeted dropwindsonde data therefore appears to provide substantial improvement to one-plane surveillance missions, but has a mixed effect on forecasts with large areal coverage. Since the targeting strategy is designed to limit error growth in partially sampled features on the edges of the sampled area, the additional areal coverage provided by the extra aircraft may shift these regions farther from the tropical cyclone so they are unlikely to negatively impact the track forecasts. One could suggest conducting all missions with more than one aircraft, but the expenses incurred also could be spent on the long-term goal of improving the data assimilation techniques so that spurious increments are not a factor.

b. Synthetic data

Aberson (2002) also showed that negative interactions between the synthetic representation of the tropical cyclone core and real data in the near-storm environment were problematic in the numerical track guidance. In the AVN vortex scheme (Lord 1991), synthetic observations describing the tropical cyclone based on current intensity, position, and motion are created. Real-time values of these parameters differ from the postprocessed best-track values due to the availability of data after operational deadlines and the ability of specialists to examine the data without time constraints. Small differences in the current storm-motion vector can lead to large forecast position differences. For example, even without amplification, a 1 m s^{-1} difference in the initial motion results in a 24-h difference in position of 86.4 km, about two-thirds of the average 24-h forecast error in the current sample. Further, if the asymmetry does not agree with the environmental flow near the storm center, an adjustment period may be required, after which the forecast may be so degraded that the dropwindsonde data cannot improve it.

As in Aberson (2002), each forecast is classified as to whether the operational storm-motion vector is either

TABLE 5. Models and forecast times for which the first listed set of track forecasts is statistically significantly better than the second set at the 95% level for the one- and multiplane samples. The ''1'' represents the single-plane sample, the ''2'' the multiplane sample. Parentheses show the cases in which the second listed version of the model is statistically significantly better than the first.

Model	12 h	24 h	36 h	48 h	72 h	84 h	96 h	108 h	120 h
GFTG/NO	1, 2	2	2		1	1	1		
GFTG/AL		2		2					
GFAL/NO	1, 2								
VBTG/NO	2	2						1	1
VBTG/AL	(1)	(1)	(1)	(1)					
VBAL/NO									
AVTG/NO	2			1	2	2			
AVTG/AL			2	2	2	2			
AVAL/NO									

''good'' or ''poor,'' with each subset having about half the total number of cases. The best-track storm-motion vector is calculated from the best-track positions at the nominal time and 6 h earlier; a storm-motion vector based on the most recent 12-h motion does not change the results. If either the direction or the speed differs by at least 15° or 3 kt, respectively, the storm-motion vector is considered to be poor. The operational and best-track storm-motion vectors for all cases are presented in Table 1.

Forecast errors of the good and poor storm-motion vector subsets of cases are presented in Fig. 8 and Table 6. GFTG forecasts are an improvement over the GFAL forecasts in the sample with good storm-motion vectors at all times except 120 h. The good storm-motion vector AVTG forecasts are better than the corresponding AVAL forecasts at all times except 48, 108, and 120 h. The VBTG forecasts in the sample with good storm-motion vectors are degraded slightly compared to the VBAL forecasts at all times except 12 h. The TG data dramatically improve the forecasts more than the AL data in the sample with poor storm-motion vectors in all three models at all times except the 12-h GFDL forecasts. Since the tropical cyclone itself is a target in every case except in Tropical Storm Alex, the requirement that the data completely surround a target region to be included in the TG data may prevent asymmetric sampling in the near-storm environment from negatively impacting the forecasts. The TG data therefore have large impact when the storm-motion vector is poor and the data either surround the tropical cyclone completely, or do not surrounded it at all, with dropwindsonde observations. This does not appear to be so important in cases in which the storm-motion vector is good, since any asymmetrical data will likely agree with the synthetic vortex data.

A new vortex technique was implemented at NCEP before the 2000 Atlantic hurricane season (Liu et al. 2000). This technique does not utilize the storm-motion vector and led to a large improvement in AVN forecast accuracy during the subsequent seasons. This new initialization scheme may allow for improvements in subsequent synoptic surveillance missions similar to those in the current good storm-motion vector sample. Improvements of the same order as those from Burpee et al. (1996) are possible in both the GFDL and AVN models in the future. Further research into targeting techniques and improvements in data assimilation likely will prove to be of benefit in future surveillance missions. No substantial changes to the sampling strategy are expected with the new vortex system since the data do not seem to negatively react with a well-defined model vortex.

7. Implications and conclusions

A strategy of subjectively finding target regions based on the NCEP bred-vector ensemble forecasting system,

TABLE 6. Models and forecast times for which the first listed set of track forecasts is statistically significantly better than the second listed set at the 95% level for the good and poor storm-motion vector samples. The G represents the good motion-vector sample, the P the poor motion vector sample. Parentheses show the cases in which the second listed version of the model is statistically significantly better than the first.

Model	12 h	24 h	36 h	48 h	72 h	84 h	96 h	108 h	120 h
GFTG/NO									
GFTG/AL	G								
GFAL/NO									
VBTG/NO									
VBAL/TG				(G)	P	P	(G)	(G)	
VBAL/NO									
AVTG/NO					G	G			
AVTG/AL									
AVAL/NO									

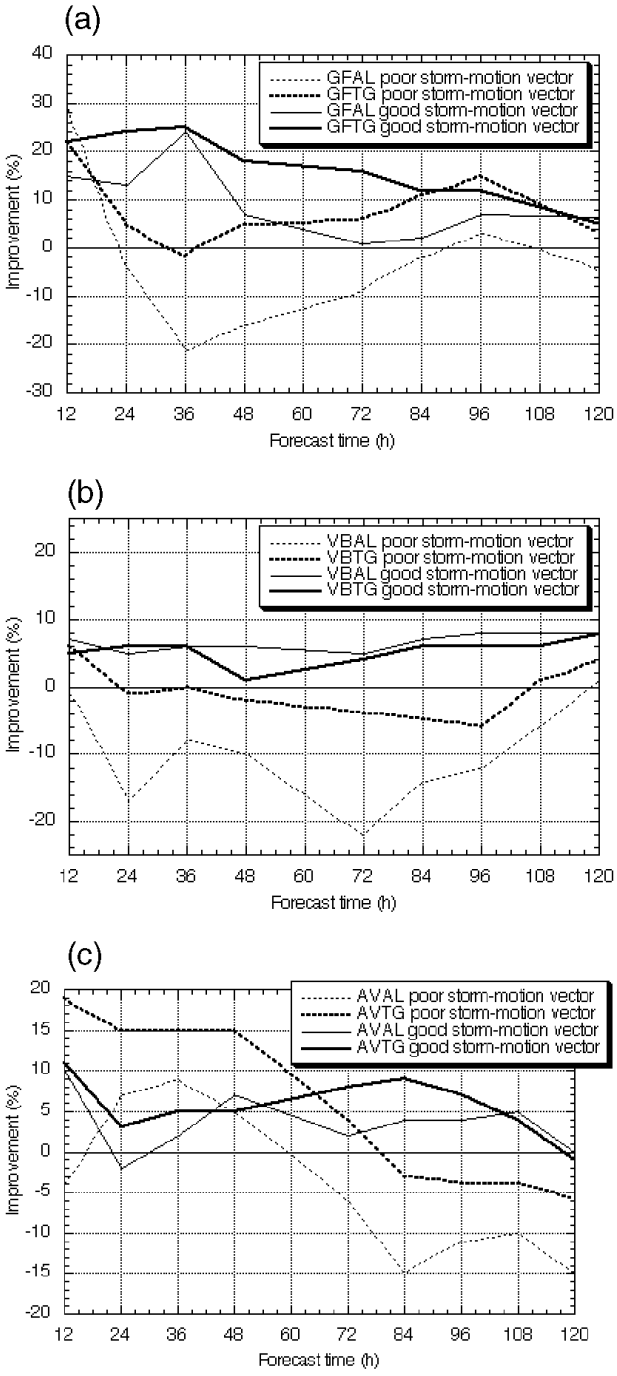

FIG. 8. As in Fig. 7, except in those cases in which the storm-motion vector was good and those in which it was poor.

and fully sampling these regions (both the extremum and completely around the edges) with regularly spaced observations, was devised. This technique produces larger forecast improvements in three dynamical tropical cyclone track forecast models than are possible by assimilating all available data from the missions examined. This result highlights the suboptimality of current data assimilation schemes, since, in an optimal scheme, the assimilation of all data would, on average, produce better results than those obtained from only a subset of data. The main region of failure of current techniques seems to be at the edges of well-sampled regions, and this may have implications for targeting strategies in extratropical wintertime situations (i.e., Szunyogh et al. 2000) in which flight tracks are often so-called kite patterns. These patterns leave such edges on both the inside and outside of the sampling patterns sometimes bisecting target regions, or sampling only the edges of these features. Further research into optimal sampling strategies is necessary to optimize flight tracks in all targeting missions.

Even larger improvements are seen with the use of the correct storm-motion vector. With the implementation of the new vortex initialization scheme in the AVN, forecast track improvements nearly as large as those seen in the original Burpee et al. (1996) synoptic flow study are possible, and preliminary results of surveillance missions since this implementation have shown this to be the case. The improvements seen in this study are as large as the regular improvement in model track forecasts seen over the last 18 yr (Aberson 2001).

Acknowledgments. The author thanks Morris Bender of GFDL, Bob Tuleya of SAIC, and Tim Marchok of SAIC working at GFDL for NCEP for help in running the GFDL hurricane model, and Jeff Ator, John Derber, Mark Iredell, Dennis Keyser, Hua-Lu Pan, and Russ Treadon of NCEP, and Jack Woollen and Bert Katz of SAIC working at NCEP, for their instruction in running the NCEP GDAS and global spectral model. Further thanks go to Tim Marchok for implementing the tropical cyclone tracking algorithm for AVN, and Maxine Brown, Janine Clements, Mickey Farley, Harold Lloyd, Mary McCann, Eric Monrad, Carolyn Pasti, George Vandenberghe, and Arthur Wick for helping in data acquistion and computer support on the NCEP computers. The support of Eugenia Kalnay of the University of Maryland and Stephen Lord of NCEP was invaluable. Sharanya Majumdar and Brian Etherton of the University of Miami and Craig Bishop of the Pennsylvania State University provided stimulating ideas and suggestions during the course of the study. Neal Dorst and Steven Feuer of HRD did much of the dropwindsonde postprocessing, and Joyce Berkeley helped draft some of the figures. Robert Kohler and William Barry provided computer support and guidance at HRD. The author also thanks the NOAA Aircraft Operations Center (AOC) flight crews and dropwindsonde operators; Sean White, former AOC G-IV project manager; HRD personnel who participated in the flights; and Naomi Surgi of NCEP. A special debt of gratitude is owed to Robert Burpee, who originated the concept of the Synoptic Flow Experiments, supported them as Director of the Hurricane Research Division, and under whose lead-

ership at the Tropical Prediction Center the operational dropwindsonde missions became a reality. The operational surveillance missions also came to fruition under the research leadership of James Franklin of NHC who drew the flight tracks and flew in nearly all missions discussed in the manuscript. The manuscript was prepared as part of the author's Ph.D. dissertation at the University of Maryland—College Park under the guidance of Professor Eugenia Kalnay.

REFERENCES

Aberson, S. D., 1998: Five-day tropical cyclone track forecasts in the North Atlantic basin. *Wea. Forecasting,* **13,** 1005–1015.

——, 2001: The ensemble of tropical cyclone track forecasting models in the North Atlantic basin (1976–2000). *Bull. Amer. Meteor. Soc.*, **82,** 1895–1904.

——, 2002: Two years of operational hurricane synoptic surveillance. *Wea. Forecasting,* **17,** 1101–1110.

——, and M. DeMaria, 1994: Verification of a nested barotropic hurricane track forecast model (VICBAR). *Mon. Wea. Rev.,* **122,** 2804–2815.

——, and J. L. Franklin, 1999: Impact on hurricane track and intensity forecasts of GPS dropwindsonde observations from the first-season flights of the NOAA Gulfstream-IV jet aircraft. *Bull. Amer. Meteor. Soc.,* **80,** 421–427.

——, S. J. Majumdar, and C. H. Bishop, 2001: A realtime ensemble for the prediction of hurricane tracks in the Atlantic basin. Preprints, *18th Conf. on Weather Analysis and Forecasting and 14th Conf. on Numerical Weather Prediction,* Fort Lauderdale, FL, Amer. Meteor. Soc., 456–457.

Appenzaler, C., H. C. Davies, J. M. Popovic, S. Nickovic, and M. B. Gavrilov, 1996: PV morphology of a frontal-wave development. *Meteor. Atmos. Phys.,* **58,** 21–40.

Bergot, T., G. Hello, A. Joly, and S. Malardel, 1999: Adaptive observations: A feasibility study. *Mon. Wea. Rev.,* **127,** 743–765.

Bishop, C. H., and Z. Toth, 1999: Ensemble transformation and adaptive observations. *J. Atmos. Sci.,* **56,** 1748–1765.

——, B. J. Etherton, and S. J. Majumdar, 2001: Adaptive sampling with the ensemble transform Kalman filter. Part I: Theoretical aspects. *Mon. Wea. Rev.,* **129,** 420–436.

Bowie, E. H., 1922: Formation and movement of West Indian hurricanes. *Mon. Wea. Rev.,* **50,** 173–190.

Bristor, C. L., 1958: Effect of data coverage on the accuracy of 500-mb forecasts. *Mon. Wea. Rev.,* **86,** 299–308.

Buizza, R., and A. Montani, 1999: Targeting observations using singular vectors. *J. Atmos. Sci.,* **56,** 2965–2985.

Burpee, R. W., J. L. Franklin, S. J. Lord, R. E. Tuleya, and S. D. Aberson, 1996: The impact of Omega dropwindsondes on operational hurricane track forecast models. *Bull. Amer. Meteor. Soc.,* **77,** 925–933.

Caplan, P., J. Derber, W. Gemmill, S.-Y. Hong, H.-L. Pan, and D. Parrish, 1997: Changes to the 1995 NCEP operational Medium-Range Forecast model analysis-forecast system. *Wea. Forecasting,* **12,** 581–594.

Chan, J. C. L., and W. M. Gray, 1982: Tropical cyclone movement and surrounding flow relationships. *Mon. Wea. Rev.,* **110,** 1354–1374.

Dong, K., and C. J. Neumann, 1986: The relationship between tropical cyclone motion and environmental geostrophic flows. *Mon. Wea. Rev.,* **114,** 115–122.

Eliassen, A., 1953: On the demands upon the aerological network from the viewpoint of numerical forecasting. *Geophysica,* **4,** 144.

Franklin, J. L., and M. DeMaria, 1992: The impact of Omega dropwindsonde observations on barotropic hurricane track forecasts. *Mon. Wea. Rev.,* **120,** 381–391.

Garriott, E. B., 1895: Tropical storms of the Gulf of Mexico and the Atlantic Ocean in September. *Mon. Wea. Rev.,* **23,** 167–169.

Gregg, W. R., 1920: Aerological observations in the West Indies. *Mon. Wea. Rev.,* **48,** 264.

Henderson, J. M., G. M. Lackmann, and J. R. Gyakum, 1999: An analysis of Hurricane Opal's forecast track errors using quasi-geostrophic potential vorticity inversion. *Mon. Wea. Rev.,* **127,** 292–307.

Hock, T. F., and J. L. Franklin, 1999: The NCAR GPS dropwindsonde. *Bull. Amer. Meteor. Soc.,* **80,** 407–420.

House, D. C., 1960: Remarks on the optimal spacing of upper-air observations. *Mon. Wea. Rev.,* **88,** 97–100.

Jordan, E. S., 1952: An observational study of the upper wind-circulation around tropical storms. *J. Meteor.,* **9,** 340–346.

Kurihara, Y., R. E. Tuleya, and M. A. Bender, 1998: The GFDL hurricane prediction system and its performance in the 1995 hurricane season. *Mon. Wea. Rev.,* **126,** 1306–1322.

Langland, R. H., and G. D. Rohaly, 1996: Adjoint-based targeting of observations for FASTEX cyclones. Preprints, *Seventh Conf. on Mesoscale Processes,* Reading, United Kingdom, Amer. Meteor. Soc., 369–371.

Larsen, R. J., and M. L. Marx, 1981: *An Introduction to Mathematical Statistics and Its Applications.* Prentice-Hall, 530 pp.

Liu, Q., T. Marchok, H.-L. Pan, M. Bender, and S. J. Lord, 2000: Improvements in hurricane initialization and forecasting at NCEP with global and regional (GFDL) models. NOAA Technical Procedures Bulletin 472, 7 pp. [Available online at http://www.nws.noaa.gov/om/tpb/472.htm.]

Lord, S. J., 1991: A bogusing system for vortex circulations in the National Meteorological Center global forecast model. Preprints, *19th Conf. on Hurricanes and Tropical Meteorology*, Miami, FL, Amer. Meteor. Soc., 328–330.

Lorenz, E. N., and K. A. Emanuel, 1998: Optimal sites for supplementary weather observations: Simulation with a small model. *J. Atmos. Sci.,* **55,** 399–414.

Miller, B. I., and P. L. Moore, 1960: A comparison of hurricane steering levels. *Bull. Amer. Meteor. Soc.,* **41,** 59–63.

Namias, J., and P. F. Clapp, 1951: Observational studies of general circulation patterns. *Compendium of Meteorology,* Amer. Meteor. Soc., 551–567.

Palmer, T. N., R. Gelaro, J. Barkmeijer, and R. Buizza, 1998: Singular vectors, metrics, and adaptive observations. *J. Atmos. Sci.,* **55,** 633–653.

Parrish, D. F., and J. C. Derber, 1992: The National Meteorological Center's spectral statistical-interpolation analysis system. *Mon. Wea. Rev.,* **120,** 1747–1763.

Pike, A. C., 1985: Geopotential heights and thicknesses as predictors of Atlantic tropical cyclone motion and intensity. *Mon. Wea. Rev.,* **113,** 931–939.

Pu, Z.-X., and E. Kalnay, 1999: Targeting observations with the quasi-linear inverse and adjoin and adjoint NCEP global models: Performance during FASTEX. *Quart. J. Roy. Meteor. Soc.,* **125,** 3329–3338.

——, ——, J. Sela, and I. Szunyogh, 1997: Sensitivity of forecast errors to initial conditions with a quasi-inverse linear model. *Mon. Wea. Rev.,* **125,** 2479–2503.

Riehl, H., and R. J. Shafer, 1944: The recurvature of tropical storms. *J. Meteor.,* **1,** 42–54.

——, W. H. Haggard, and R. W. Sanborn, 1956: On the prediction of 24-hour hurricane motion. *J. Meteor.,* **13,** 415–420.

Shapiro, L. J., 1996: The motion of Hurricane Gloria: A potential vorticity diagnosis. *Mon. Wea. Rev.,* **124,** 2497–2508.

——, and J. L. Franklin, 1999: Potential vorticity asymmetries and tropical cyclone motion. *Mon. Wea. Rev.,* **127,** 124–131.

Simpson, R. H., 1971: The decision process in hurricane forecasting. NOAA Tech. Memo. NWS SR-53, 30 pp.

Surgi, N., H.-L. Pan, and S. J. Lord, 1998: Improvement of the NCEP global model over the Tropics: An evaluation of model performance during the 1995 hurricane season. *Mon. Wea. Rev.,* **126,** 1287–1305.

Szunyogh, I., Z. Toth, R. E. Morss, S. J. Majumdar, B. J. Etherton, and C. H. Bishop, 2000: The effect of targeted dropsonde ob-

servations during the 1999 winter storms reconnaissance program. *Mon. Wea. Rev.*, **128,** 3520–3537.
Toth, Z., and E. Kalnay, 1993: Ensemble forecasting at NMC: The generation of perturbations. *Bull. Amer. Meteor. Soc.*, **74,** 2317–2330.
Tuleya, R. E., and S. J. Lord, 1997: The impact of dropwindsonde data on GFDL hurricane model forecasts using global analyses. *Wea. Forecasting,* **12,** 307–323.
U.S. Weather Bureau, 1892: Some observations of the wind direction at different altitudes around West India cyclones. *Mon. Wea. Rev.,* **20,** 50–51.
Velden, C. S., and L. M. Leslie, 1991: The basic relationship between tropical cyclone intensity and the depth of the environmental steering layer in the Australian region. *Wea. Forecasting,* **6,** 244–253.
Viñes, B., 1898: Investigation of the cyclonic circulation and the translatory movement of West Indian hurricanes. Rep. W. B. 168, U.S. Dept. of Agriculture Weather Bureau, 34 pp.
Woollen, J. R., 1991: New NMC operational OI quality control. Preprints, *Ninth Conf. on Numerical Weather Prediction,* Denver, CO, Amer. Meteor. Soc., 24–27.